Diagnostic Accuracy Study

Medicine®

OPEN

Using arterial spin labeling blood flow and its histogram analysis to distinguish early-stage nasopharyngeal carcinoma from lymphoid hyperplasia

Bohan Xiao, BS[a], Peiguo Wang, MD[b], Yingru Zhao, MD[a], Ying Liu, MD[a], Zhaoxiang Ye, MD[a,*]

Abstract

To investigate the feasibility of arterial spin labeling (ASL) blood flow (BF) and its histogram analysis to distinguish early-stage nasopharyngeal carcinoma (NPC) from nasopharyngeal lymphoid hyperplasia (NPLH).

Sixty-three stage T1 NPC patients and benign NPLH patients underwent ASL on a 3.0-T magnetic resonance imaging system. BF histogram parameters were derived automatically, including the mean, median, maximum, minimum, kurtosis, skewness, and variance. Absolute values were obtained for skewness and kurtosis (absolute value of skewness [AVS] and absolute value of kurtosis [AVK], respectively). The Mann–Whitney *U* test, receiver operating characteristic curve, and multiple logistic regression models were used for statistical analysis.

The mean, maximum, and variance of ASL BF values were significantly higher in early-stage NPC than in NPLH (all $P < 0.0001$), while the median and AVK values of early-stage NPC were also significantly higher than those of NPLH (all $P < 0.001$). No significant difference was found between the minimum and AVS values in early-stage NPC compared with NPLH ($P = 0.125$ and $P = 0.084$, respectively). The area under the curve (AUC) of the maximum was significantly higher than those of the mean and median ($P < 0.05$). The AUC of variance was significantly higher than those of the other parameters (all $P < 0.05$). Multivariate analysis showed that variance was the only independent predictor of outcome ($P < 0.05$).

ASL BF and its histogram analysis could distinguish early-stage NPC from NPLH, and the variance value was a unique independent predictor.

Abbreviations: ASL = arterial spin labeling, AUC = area under the curve, AVK = absolute value of kurtosis, AVS = absolute value of skewness, BF = blood flow, DCE-MRI = dynamic contrast-enhanced magnetic resonance imaging, DWI = diffusion-weighted imaging, FOV = field of view, IVIM = intravoxel incoherent motion, MRI = magnetic resonance imaging, NPC = nasopharyngeal carcinoma, NPLH = nasopharyngeal lymphoid hyperplasia, PLD = postlabeling delay, ROC = receiver-operating characteristic, ROI = region of interest.

Keywords: arterial spin labeling, histogram, nasopharyngeal carcinoma, nasopharyngeal lymphoid hyperplasia

1. Introduction

Nasopharyngeal carcinoma (NPC) is one of the most common malignant head and neck tumors in Southern China and Southeast Asia, with a reported incidence of 10–30/100,000 population per year.[1] Unlike advanced-stage NPC, early-stage NPC lacks clinical symptoms and is usually detected as an incidental finding on head and neck or brain imaging. In NPC endemic regions, more early-stage NPC cases can be found by screening. Early-stage NPC appears as regional soft tissue thickening without deep invasion. It needs to be differentiated from benign nasopharyngeal lymphoid hyperplasia (NPLH), which is caused by nasopharyngeal inflammation and lymphoid hyperplasia.[2]

Endoscopic biopsy is the gold standard to confirm early-stage NPC.[3] However, the results may sometimes be false negative due to the lack of tumor cells in the obtained tissues or the superficial inflammation of the tumor. Moreover, as an invasive examination with the risk of bleeding, the use of endoscopic biopsy is limited in the clinical setting.[4] Conventional magnetic resonance imaging (MRI) has been regarded as the optimal imaging modality for the nasopharynx because of its excellent soft tissue contrast resolution. Previous studies demonstrated that

Editor: Neeraj Lalwani.

This study was supported by the Natural Science Foundation of Tianjin (grant number: 17JCYBJC26600).

The authors have no conflicts of interest to disclose.

The datasets generated during and/or analyzed during the current study are available from the corresponding author on reasonable request.

[a] Department of Radiology, [b] Department of Radiotherapy, Tianjin Medical University Cancer Institute and Hospital, National Clinical Research Center for Cancer, Key Laboratory of Cancer Prevention and Therapy, Tianjin, China.

[*] Correspondence: Zhaoxiang Ye, Department of Radiology, Tianjin Medical University Cancer Institute and Hospital, Huan-Hu-Xi Road, Ti-Yuan-Bei, He Xi District, Tianjin 300060, China (e-mail: yezhaoxiang@163.com).

How to cite this article: Xiao B, Wang P, Zhao Y, Liu Y, Ye Z. Using arterial spin labeling blood flow and its histogram analysis to distinguish early-stage nasopharyngeal carcinoma from lymphoid hyperplasia. Medicine 2021;100:8 (e24955).

Received: 29 May 2020 / Received in final form: 9 October 2020 / Accepted: 4 February 2021

http://dx.doi.org/10.1097/MD.0000000000024955

diffuse wall thickening, vertical stripes, symmetry, and homogeneous enhancement were common MR features of NPLH, whereas focal mass, loss of adenoidal stripes, and inhomogeneous enhancement tend to be characteristic of early-stage NPC.[5] Nevertheless, there is still some confusion, especially when the morphological features are atypical or overlap between benign and malignant lesions.[2,6]

Angiogenesis is one of the most important factors for malignant tumor growth and invasion.[7,8] Newly formed tumor vasculatures are abnormal in structure and function, leading to increased blood flow (BF) and permeability, which could be reflected by hyperperfusion on MR perfusion assessments. Currently, perfusion information can be acquired by invasive or noninvasive MRI approaches. Dynamic contrast-enhanced magnetic resonance imaging (DCE-MRI) has been used as a standard approach to obtain both anatomical and perfusion information and is confirmed to be helpful in differentiating benign from malignant tumors.[9–11] However, DCE-MRI cannot be performed without injecting exogenous contrast media, which restricts its application, especially in screening. Intravoxel incoherent motion (IVIM) diffusion-weighted imaging (DWI) is noninvasive and can provide both diffusion and perfusion information for tissue characterization without the use of exogenous contrast. Recent studies[12,13] reported that IVIM could distinguish NPC from enlarged adenoids in the nasopharynx and is promising in early-stage NPC screening. It should be noted that IVIM is based on echo-planar imaging acquisition, which is prone to be unsuccessful due to the severe image degradation caused by physiological motion artifacts or magnetic field heterogeneities at the air–bone or air–soft tissue interfaces around the skull base.

Arterial spin labeling (ASL) is another noninvasive MR perfusion approach. It utilizes magnetically labeled water protons in the blood as an endogenous contrast agent to achieve perfusion imaging and avoid issues associated with contrast media administration. The parameters of BF, which can be measured by ASL, can reflect physiological information about tissue perfusion. Applications of ASL have been reported primarily in the central nervous system.[14–17] Recently, some studies have discussed the role of ASL in head and neck cancer, including in differential diagnosis, staging, and monitoring of the response to therapy.[18–20] However, to our knowledge, there are only a few studies about the applications of ASL in NPC.[21,22]

The purpose of this study was to investigate the feasibility of the use of parameters derived from ASL BF and its histogram analysis to distinguish early-stage NPC from NPLH.

2. Materials and methods

2.1. Patient population

This prospective study was approved by the ethics committee of the hospital. All recruited patients provided written informed consent. All the patients were performed a MRI examination first, followed by an endoscopic biopsy. The biopsy site was determined with reference to MRI findings. Between July 2018 and December 2019, 63 consecutive newly diagnosed (first episode) stage T1 NPC patients and benign NPLH patients were enrolled in this study. All recruited patients eligible for this study met the following criteria: biopsy-proven diagnosis of stage T1 NPC or benign NPLH; no history of prior chemotherapy, radiotherapy, or other treatments; no contraindications to MR examinations; and nasopharyngeal thickening > 5 mm in size.

2.2. MR imaging techniques

MR imaging examinations of the whole nasopharynx were performed with a 3.0-T whole-body system (Discovery MR750; GE Medical Systems, Milwaukee, WI) utilizing an 8-channel head and neck phased-array coil. The imaging protocol included the following: axial T1-weighted images (fast spin-echo [FSE]): repetition time/echo time (TR/TE) = 700/10 ms, number of excitations (NEX) = 2, bandwidth = 50 kHz, thickness = 6 mm, slice gap = 1 mm, field of view (FOV) = 28 cm, matrix = 288 × 192; axial T2-weighted images with fat suppression (fast recovery fast spin-echo [FRFSE]): TR/TE = 5000/70 ms, NEX = 3, bandwidth = 41.7 kHz, thickness = 6 mm, slice gap = 1 mm, FOV = 28 cm, matrix = 288 × 224; axial periodically rotated overlapping parallel lines with enhanced reconstruction (PROPELLER) DWI: TR/TE = 4300/70 ms, NEX = 1.5, bandwidth = 83.3 kHz, thickness = 6 mm, slice gap = 1 mm, FOV = 28 cm, matrix = 128 × 128, b values of 0 and 1000 s/mm2; and axial ASL (3D fast spin-echo spiral-based pseudocontinuous pCASL sequence): TR/TE = 4500/10 ms, NEX = 3, bandwidth = 62.5 kHz, thickness = 4 mm, slice gap = 0 mm, FOV = 26 cm, postlabeling delay (PLD) = 1525 ms.

2.3. Image analysis

All ASL images were transferred to the Advantage Workstation, and Functool software (ADW 4.6 version; GE Medical Systems, Milwaukee, WI) was used for postprocessing analyses. The ASL images were corrected for motion, and the labeled images were pairwise subtracted from the unlabeled images and then averaged to generate the mean difference image (ΔM). Quantitative BF (f) maps were calculated based on the following equation[2,3]:

$$f = \lambda \Delta M R_{1a} / 2 a M_0 [\exp(-w R_{1a}) - \exp(-(\tau + w) R_{1a})]$$

where $R_{1\boxtimes}$ (0.61 s^{-1} at 3 T) is the longitudinal relaxation rate of blood, M_0 is the equilibrium magnetization of brain tissue, ⊠ (=0.8) is the tagging efficiency, τ (=1.5 s) is the duration of the labeling pulse, w (=2 s) is the PLD time, and λ (=0.9 g/mL) is the blood/tissue water partition coefficient.

In all cases, BF maps were saved in DICOM format and processed offline with custom-made MATLAB-based applications (Omni Kinetics; GE Healthcare, Beijing, China) on a standard Windows operating system. The regions of interest (ROIs) covered as much of the lesion as possible on the slice with the maximum NPC or NPLH, while avoiding large necrotic, cystic, and hemorrhagic areas by referencing the T1WI and T2WI images. All measures were performed by 1 radiologist (YR Zhao, MD) with 15 years of experience in head and neck radiology. The radiologist was blinded to the pathology results. Based on the ROIs, the following BF histogram parameters were derived automatically: mean, median, maximum, minimum, kurtosis, skewness, and variance. Absolute values were obtained for skewness and kurtosis (AVS and absolute value of kurtosis [AVK], respectively).

2.4. Statistical analysis

The parameters are expressed as the mean (± standard deviation) and were compared between early-stage NPC and NPLH with the Mann–Whitney U test. The ability to discriminate benign and malignant lesions was quantified by the area under the curve (AUC) of the receiver operating characteristic (ROC) curve. The respective cut-off values of each parameter were determined to

Table 1

Analysis of ASL BF histogram parameters in early-stage NPC and NPLH.

Parameters	Early-stage NPC	NPLH	*P* value
Mean	70.89 ± 25.24	48.86 ± 12.29	0.000
Median	73.59 ± 28.45	53.24 ± 14.68	0.004
Maximum	127.88 ± 46.03	80.68 ± 19.24	0.000
Minimum	22.73 ± 10.09	18.41 ± 9.07	0.099
AVS	0.34 ± 0.32	0.45 ± 0.28	0.084
AVK	0.83 ± 0.42	0.53 ± 0.35	0.007
Variance	519.53 ± 332.02	145.04 ± 85.06	0.000

ASL = arterial spin labeling, AVK = absolute value of kurtosis, AVS = absolute value of skewness, BF = blood flow, NPC = nasopharyngeal carcinoma, NPLH = nasopharyngeal lymphoid hyperplasia.

achieve the best diagnostic accuracy. The ROC curves were compared using the DeLong method. Finally, the parameters were subsequently analyzed by multiple logistic regression models to determine their independent predictive values. Statistical analyses were performed with SPSS (version 21; IBM SPSS, Chicago, IL) and MedCalc (version 15.8; MedCalc, Mariakerke, Belgium). A P value of < 0.05 was considered a significant difference.

3. Results

Among the 63 patients, 41 patients had early-stage NPC (25 males and 16 females; mean age 52.8 years, range 27–77 years) and 22 patients had NPLH (10 males and 12 females; mean age 36.2 years, range 18–63 years). The ASL BF histogram parameters in both early-stage NPC and NPLH are shown in Table 1 and Figure 1. The mean, maximum, and variance of ASL BF values were significantly higher in early-stage NPC than in NPLH (all $P < 0.0001$), while the median and AVK values of early-stage NPC were also significantly higher than those of NPLH (all $P < 0.001$). No significant difference was found between the minimum and AVS values in early-stage NPC compared with NPLH ($P = 0.099$ and $P = 0.084$, respectively). The MR images for representative early-stage NPC and NPLH patients are shown in Figures 2 and 3.

The results of ROC analysis for the above-listed significant ASL BF values to distinguish malignant from benign lesions are summarized in Table 2 and Figure 4. The AUC of the maximum was significantly higher than those of the mean and median ($P < 0.05$). Variance showed optimal performance in discriminating between early-stage NPC and NPLH (cut-off value, 300.8; AUC, 0.924; sensitivity, 80.49%; specificity, 95.45%). The AUC of variance was significantly higher than those of the other parameters (all $P < 0.05$). Multivariate analysis showed that variance was the only independent predictor of outcome ($P < 0.05$).

4. Discussion

To the best of our knowledge, this is the first study to distinguish early-stage NPC from NPLH using ASL BF and histogram analysis. In this study, we found that the mean, maximum, median, variance, and AVK of ASL BF histogram values in early-stage NPC were significantly higher than those in NPLH, showing potential value in discriminating early-stage NPC from NPLH. Variance achieved the highest AUC (0.924) and was the only independent diagnostic parameter for the differentiation of early-stage NPC and NPLH.

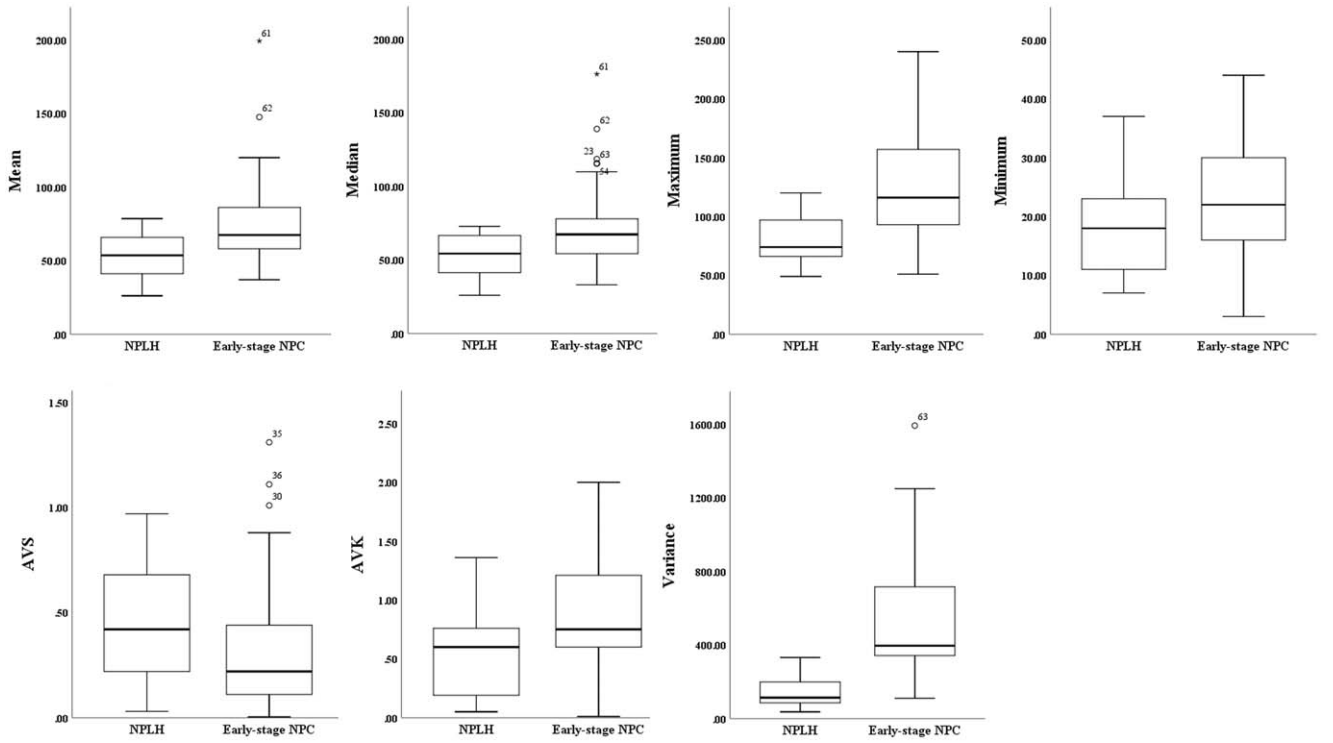

Figure 1. Boxplots show ASL BF histogram parameters for early-stage NPC and NPLH. The lines in the boxes indicate medians, and the boundaries of the boxes indicate lower and upper quartiles. Outliers are plotted as individual points. ASL = arterial spin labeling, BF = blood flow, NPC = nasopharyngeal carcinoma, NPLH = nasopharyngeal lymphoid hyperplasia.

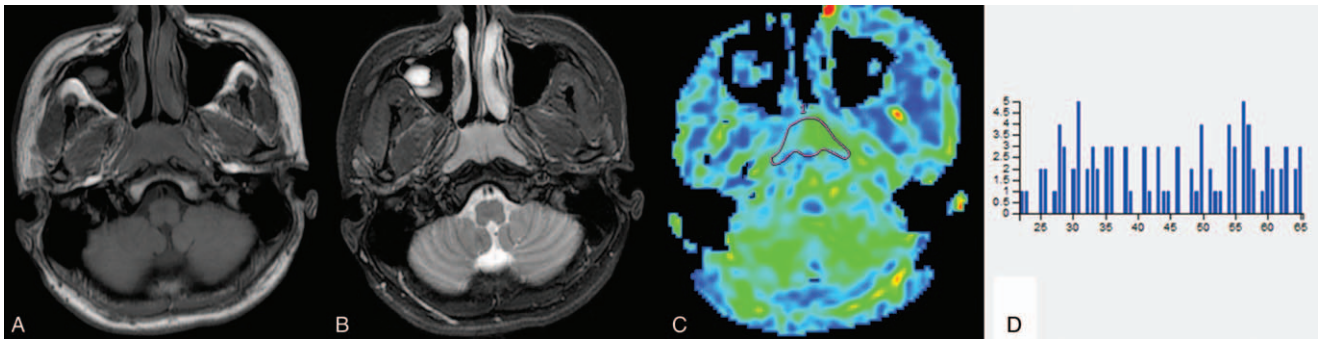

Figure 2. A 23-year-old male with NPLH. Axial T1-weighted image (A) and T2-weighted image (B) show diffuse symmetrical nasopharyngeal mucosal thickening. On the ASL BF map (C), a polygonal ROI was manually delineated with reference to T1WI and T2WI, and the NPLH exhibited homogeneous lower perfusion. In the BF histogram (D), the abscissa represents different BF values within the ROI, the ordinate represents the occurrence frequency of each BF value, and the parameters are as follows: mean = 44.84, median = 46.1, max = 65, min = 22, AVS = 0.05, AVK = 1.40, and variance = 163.18. AVK = absolute value of kurtosis, BF = blood flow, ROI = region of interest.

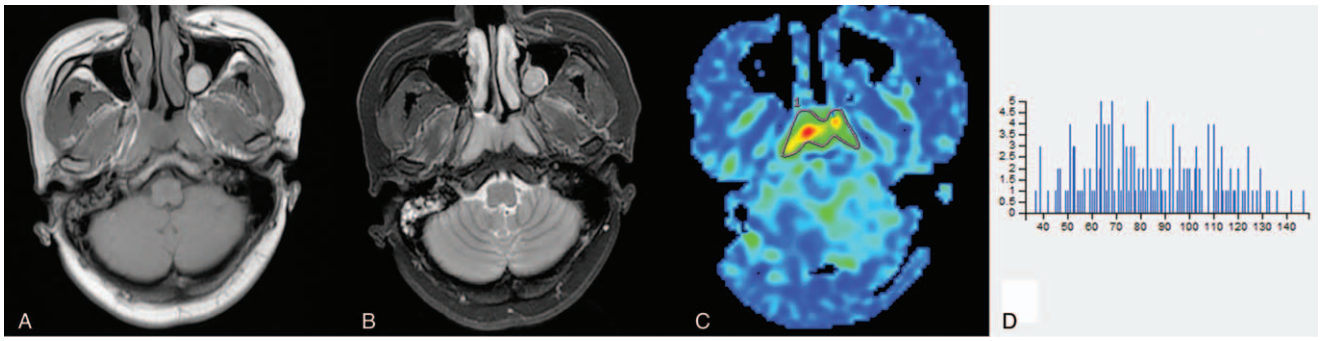

Figure 3. A 48-year-old female with early-stage NPC. Axial T1-weighted image (A) and T2-weighted image (B) show diffuse symmetrical nasopharyngeal mucosal thickening. On the ASL BF map (C), a polygonal ROI was manually delineated with reference to T1WI and T2WI, and the NPC lesion exhibited inhomogeneous higher perfusion. In the BF histogram (D), the abscissa represents different BF values within the ROI, the ordinate represents the occurrence frequency of each BF value, and the parameters are as follows: mean = 84.41, median = 81.84, max = 150, min = 33, AVS = 0.31, AVK = 0.72, and variance = 710.97.

Tumor blood flow is one of the most important biological markers for the assessment of tumor viability because it reflects neovascularity and hyperperfusion and is considered a key mechanism in tumor growth and malignancy.[19,24] NPC is a hypervascular tumor with abundant newly formed vessels that are structurally and functionally abnormal. Compared with normal tissues, malignant tumors grow more rapidly. For growth, tumors rely on the transport of a large amount of nutrients and oxygen to the tumor site. This nutrient flow is facilitated by the growth of new blood vessels. In contrast to normal blood vessels, the newly generated blood vessels are larger in size and have incomplete vessel walls, leading to increased BF and vascular permeability. Therefore, the perfusion level of tumor tissue is significantly higher than that of normal tissue.

ASL could measure tissue BF noninvasively to evaluate angiogenesis in vivo. Previous studies have demonstrated that ASL performs well in differentiating malignant from benign tumors and can be an alternative to contrast agent perfusion.[25–28] In this study, the mean, maximum, and median ASL BF values showed significant differences between early-stage NPC and NPLH, and the AUC of the maximum was significantly higher than those of the mean and median ($P < 0.05$). This finding

Table 2

Diagnostic performance of ASL BF histogram parameters in distinguishing early-stage NPC from NPLH.

Parameters	AUC	Cut-off value	Sensitivity (%) (95% CI)	Specificity (%) (95% CI)	Pos LR (95% CI)	Neg LR (95% CI)	*P* value
Mean	0.729	53.8	85.37 (70.8–94.4)	54.55 (32.2–75.6)	1.88 (1.2–3.0)	0.27 (0.1–0.6)	0.0007
Median	0.721	52.1	85.37 (70.8–94.4)	50.00 (28.2–71.8)	1.71 (1.1–2.6)	0.29 (0.1–0.7)	0.0010
Maximum	0.841	105	60.98 (44.5–75.8)	90.91 (70.8–98.9)	6.71 (1.7–25.7)	0.43 (0.3–0.6)	<0.0001
AVK	0.707	0.98	41.46 (26.3–57.9)	95.45 (77.2–99.9)	9.12 (1.3–64.1)	0.61 (0.5–0.8)	0.0025
Variance	0.924	300.8	80.49 (65.1–91.2)	95.45 (77.2–99.9)	17.71 (2.6–120.9)	0.20 (0.1–0.4)	<0.0001

ASL = arterial spin labeling, AUC = area under the receiver operating characteristic curve, AVK = absolute value of kurtosis, BF = blood flow, CI = confidence interval, Neg LR = negative likelihood ratio, NPC = nasopharyngeal carcinoma, NPLH = nasopharyngeal lymphoid hyperplasia, Pos LR = positive likelihood ratio.

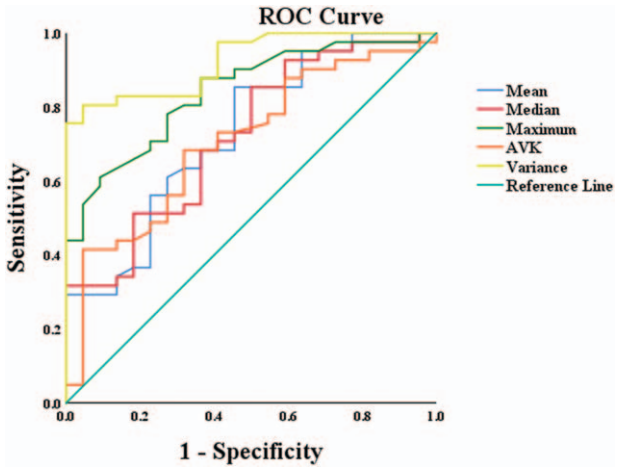

Figure 4. ROC curve analysis of ASL BF histogram parameters with respective areas under the curves in distinguishing early-stage NPC from NPLH. ROC = receiver-operating characteristic.

indicated that the maximum ASL BF value may promote more accurate differentiation between early-stage NPC and NPLH than the mean and median ASL BF values. This may be because the maximum ASL BF value is derived from the hottest spot regions, reflecting the greatest difference in perfusion level between the 2 disease entities. Unlike DCE-MRI perfusion, ASL utilizes magnetically labeled water protons in the blood as an endogenous contrast agent, which is more diffusible than the contrast media in DCE-MRI perfusion (gadolinium chelate), and its BF measurements might be more accurate.[18] In addition, ASL can be performed safely to avoid issues associated with contrast media administration, making it especially suitable for early-stage NPC screening. However, in ASL perfusion, the PLD time, which refers to the waiting time for the blood to transit from the labeling site to the imaging slice, may lead to potential inaccurate estimations of BF caused by individual differences in circulation.[17,25]

Vascular heterogeneity is one of the most important biological features of malignant tumors[29,30] and can also be seen on the ASL BF map.[19,26] There are large differences in the diameter, morphology, and density of microvessels in malignant tumors, and microscopic necrotic areas frequently occur in malignant tumors, which can be considered the reason for heterogeneity on the ASL BF map. Therefore, compared with NPLH, more inhomogeneous perfusion was frequently observed on the ASL BF map of early-stage NPC. Conventional mean and median quantitative measures cannot reveal the difference between the 2 disease entities in spatial heterogeneity.

Histogram analysis is a mathematical method that can provide more information about tissue heterogeneity. Numerous studies have suggested its value in tumor diagnosis, grading, staging, and prognosis prediction in various organs.[31–34] Several studies have used ASL BF and its histogram analysis in glioma grading and sinonasal tumor differentiation.[35,36] The AVK, AVS, and variance of histogram parameters reflect the extent of deviation from a normal distribution.[37] In this study, the variance value was the unique independent predictor of early-stage NPC indicated by the multivariate logistic regression analysis ($P < 0.05$). This result indicated that the variance value could reflect the heterogeneity of tissue perfusion on the ASL BF map and plays an important role in distinguishing early-stage NPC from NPLH. A previous study[13] of IVIM indicated that D and $ADC_{300-1000}$ mean could distinguish early-stage NPC from NPLH. However, IVIM performed in the nasopharynx has a high failure rate of approximately 10%, limiting its use in clinical applications. Compared with that in IVIM images, severe image degradation around the skull base was less frequent on ASL BF maps owing to the immunity of ASL sequences to field inhomogeneity. Therefore, ASL BF and its histogram analysis can be performed more successfully in the nasopharynx.

There were several limitations of this study. First, the sample size was relatively small. Second, this study did not correlate ASL BF and its histogram analysis with histological features. Third, only one PLD time in ASL was used, which may not be suitable for some cases. Fourth, the ROIs were drawn on only the slice with the maximum NPC or NPLH but not on all lesion slices. Therefore, in the future, by recruiting more patients, correlating ASL BF and its histogram analysis with histological features, and applying multi-PLD ASL protocols and whole lesion ROIs, the value of this diagnostic imaging method will increase.

5. Conclusions

In conclusion, the present study demonstrated that ASL BF and its histogram analysis could distinguish early-stage NPC from NPLH, and the variance value was a unique independent predictor. As a noncontrast perfusion method, ASL can be used safely and successfully in the nasopharynx and is especially suitable for early-stage NPC screening.

Acknowledgments

The authors thank Qin Wang, Fengkui Wang, Di Feng, Xiaoyu Yin, and Dongzhen Long for technical support and Qian Li and Wei Li for language editing.

Author contributions

Conceptualization: Bohan Xiao.
Data curation: Bohan Xiao, Ying Liu.
Formal analysis: Bohan Xiao, Ying Liu.
Funding acquisition: Bohan Xiao.
Investigation: Peiguo Wang.
Methodology: Bohan Xiao, Zhaoxiang Ye.
Project administration: Bohan Xiao, Peiguo Wang.
Resources: Peiguo Wang.
Software: Yingru Zhao.
Supervision: Zhaoxiang Ye.
Validation: Zhaoxiang Ye.
Visualization: Yingru Zhao.
Writing – original draft: Bohan Xiao.
Writing – review & editing: Yingru Zhao, Ying Liu.

References

[1] Lai V, Khong PL. Updates on MR imaging and 18 F-FDG PET/CT imaging in nasopharyngeal carcinoma. Oral Oncol 2014;50:539–48.
[2] Wang ML, Wei XE, Yu MM, et al. Value of contrast-enhanced MRI in the differentiation between nasopharyngeal lymphoid hyperplasia and T1 stage nasopharyngeal carcinoma. Radiol Med 2017;122:743–51.
[3] Chan AT, Felip E. Nasopharyngeal cancer: ESMO clinical recommendations for diagnosis, treatment and follow-up. Ann Oncol 2009;20 (suppl 4):123–5.

[4] King AD, Vlantis AC, Bhatia KSS, et al. Primary nasopharyngeal carcinoma: diagnostic accuracy of MR imaging versus that of endoscopy and endoscopic biopsy. Radiology 2011;258:531–7.
[5] King AD, Wong LYS, Law BKH, et al. MR imaging criteria for the detection of nasopharyngeal carcinoma: discrimination of early-stage primary tumors from benign hyperplasia. AJNR Am J Neuroradiol 2018;39:515–23.
[6] King AD, Vlantis AC, Yuen TW, et al. Detection of nasopharyngeal carcinoma by MR imaging: diagnostic accuracy of MRI compared with endoscopy and endoscopic biopsy based on long-term follow-up. Am J Neuroradiol 2015;36:2380–5.
[7] Fukumura D, Jain RK. Imaging angiogenesis and the microenvironment. APMIS 2008;116:695–715.
[8] Abdel Razek AA, Gaballa G. Role of perfusion magnetic resonance imaging in cervical lymphadenopathy. J Comput Assist Tomogr 2011;35:21–5.
[9] Li X, Hu JL, Zhu LM, et al. The clinical value of dynamic contrast-enhanced MRI in differential diagnosis of malignant and benign ovarian lesions. Tumour Biol 2015;36:5515–22.
[10] Liu X, Cheng D, Wang W. MRI in differentiation of benign and malignant tongue tumors. Front Biosci (Landmark Ed) 2015;20: 614–20.
[11] Cheng Z, Wu Z, Shi G, et al. Discrimination between benign and malignant breast lesions using volumetric quantitative dynamic contrast-enhanced MR imaging. Eur Radiol 2018;28:982–91.
[12] Zhang SX, Jia QJ, Zhang ZP, et al. Intravoxel incoherent motion MRI: emerging applications for nasopharyngeal carcinoma at the primary site. Eur Radiol 2014;24:1998–2004.
[13] Ai QY, King AD, Chan JSM, et al. Distinguishing early-stage nasopharyngeal carcinoma from benign hyperplasia using intravoxel incoherent motion diffusion-weighted MRI. Eur Radiol 2019;29: 5627–34.
[14] Telischak NA, Detre JA, Zaharchuk G. Arterial spin labeling MRI: clinical applications in the brain. J Magn Reson Imaging 2015;41: 1165–80.
[15] Haller S, Zaharchuk G, Thomas DL, et al. Arterial spin labeling perfusion of the brain: emerging clinical applications. Radiology 2016;281:337–56.
[16] Kong L, Chen H, Yang Y, et al. A meta-analysis of arterial spin labelling perfusion values for the prediction of glioma grade. Clin Radiol 2017;72:255–61.
[17] Abdel Razek AAK, Talaat M, El-Serougy L, et al. Clinical applications of arterial spin labeling in brain tumors. J Comput Assist Tomogr 2019;43:525–32.
[18] Fujima N, Kudo K, Yoshida D, et al. Arterial spin labeling to determine tumor viability in head and neck cancer before and after treatment. J Magn Reson Imaging 2014;40:920–8.
[19] Fujima N, Kudo K, Tsukahara A, et al. Measurement of tumor blood flow in head and neck squamous cell carcinoma by pseudo-continuous arterial spin labeling: comparison with dynamic contrast-enhanced MRI. J Magn Reson Imaging 2015;41:983–91.
[20] Abdel Razek AAK, Nada N. Arterial spin labeling perfusion-weighted MR imaging: correlation of tumor blood flow with pathological degree of tumor differentiation, clinical stage and nodal metastasis of head and neck squamous cell carcinoma. Eur Arch Otorhinolaryngol 2018;275: 1301–7.
[21] Lin M, Yu X, Ouyang H, et al. Consistency of T2WI-FS/ASL fusion images in delineating the volume of nasopharyngeal carcinoma. Sci Rep 2015;5:18431.
[22] Lin M, Yu X, Luo D, et al. Investigating the correlation of arterial spin labeling and dynamic contrast enhanced perfusion in primary tumor of nasopharyngeal carcinoma. Eur J Radiol 2018;108:222–9.
[23] Wu WC, Fernández-Seara M, Detre JA, et al. A theoretical and experimental investigation of the tagging efficiency of pseudo continuous arterial spin labeling. Magn Reson Med 2007;58:1020–7.
[24] Barrett T, Brechbiel M, Bernardo M, et al. MRI of tumor angiogenesis. J Magn Reson Imaging 2007;26:235–49.
[25] Xu Q, Liu Q, Ge H, et al. Tumor recurrence versus treatment effects in glioma: a comparative study of three dimensional pseudo-continuous arterial spin labeling and dynamic susceptibility contrast imaging. Medicine (Baltimore) 2017;96:e9332.
[26] Xu L, Xu L, Zhu H. Evaluation of three-dimensional arterial spin labeling perfusion imaging for the pathological investigation of musculoskeletal tumors. Exp Ther Med 2018;15:5029–34.
[27] Razek AAKA. Multi-parametric MR imaging using pseudo-continuous arterial-spin labeling and diffusion-weighted MR imaging in differentiating subtypes of parotid tumors. Magn Reson Imaging 2019;63:55–9.
[28] Ye J, Xu Q, Wang SA. Differentiation between fat-poor angiomyolipoma and clear cell renal cell carcinoma: qualitative and quantitative analysis using arterial spin labeling MR imaging. Abdom Radiol (NY) 2020;45:512–9.
[29] Türkbey B, Thomasson D, Pang Y, et al. The role of dynamic contrast-enhanced MRI in cancer diagnosis and treatment. Diagn Interv Radiol 2010;16:186–92.
[30] Zheng D, Chen Y, Chen Y, et al. Dynamic contrast-enhanced MRI of nasopharyngeal carcinoma: a preliminary study of the correlations between quantitative parameters and clinical stage. J Magn Reson Imaging 2014;39:940–8.
[31] Xu XQ, Ma G, Wang YJ, et al. Histogram analysis of diffusion kurtosis imaging of nasopharyngeal carcinoma: correlation between quantitative parameters and clinical stage. Oncotarget 2017;8:47230–8.
[32] Park M, Kim J, Choi YS, et al. Application of dynamic contrast-enhanced MRI parameters for differentiating squamous cell carcinoma and malignant lymphoma of the oropharynx. AJR Am J Roentgenol 2016;206:401–7.
[33] Surov A, Ginat DT, Lim T, et al. Histogram Analysis parameters apparent diffusion coefficient for distinguishing high and low-grade meningiomas: a multicenter study. Transl Oncol 2018;11:1074–9.
[34] Kondo M, Uchiyama Y. Apparent diffusion coefficient histogram analysis for prediction of prognosis in glioblastoma. J Neuroradiol 2018;45:236–41.
[35] Arisawa A, Watanabe Y, Tanaka H, et al. Comparative study of pulsed-continuous arterial spin labeling and dynamic susceptibility contrast imaging by histogram analysis in evaluation of glial tumors. Neuroradiology 2018;60:599–608.
[36] Fujima N, Kameda H, Tsukahara A, et al. Diagnostic value of tumor blood flow and its histogram analysis obtained with pCASL to differentiate sinonasal malignant lymphoma from squamous cell carcinoma. Eur J Radiol 2015;84:2187–93.
[37] Wu G, Xie R, Li Y, et al. Histogram analysis with computed tomography angiography for discriminating soft tissue sarcoma from benign soft tissue tumor. Medicine (Baltimore) 2020;99:e18742.